Available online at www.sciencedirect.com
SCIENCE DIRECT®
International Journal of Mass Spectrometry 238 (2004) 287–297
International Journal of Mass Spectrometry
www.elsevier.com/locate/ijms

Microstructural and conformational studies of polyether copolymers

Anthony T. Jackson[a,*], James H. Scrivens[a], Jonathan P. Williams[b,1], Erin Shammel Baker[c], Jennifer Gidden[c], Michael T. Bowers[c]

[a] *ICI Measurement Science Group, Wilton Centre, Wilton, Redcar, Cleveland TS10 4RF, UK*
[b] *Waters MS Technologies, Atlas Park, Simonsway, Manchester M22 5PP, UK*
[c] *Department of Chemistry and Biochemistry, University of California, Santa Barbara, CA 93106-9510, USA*

Received 10 September 2004; accepted 27 September 2004

Abstract

A combined structural/conformational study of ethylene oxide/propylene oxide (EO/PO) copolymers has been undertaken. Electrospray ionisation (ESI) and matrix-assisted laser desorption/ionisation (MALDI) methods have been utilised and ESI-tandem mass spectrometry (MS/MS) product ion spectra, including accurate mass measurements, utilised to establish fragmentation pathways. This has enabled end group and sequence information to be obtained. Ion mobility mass spectrometry experimental, along with theoretical, approaches has been used in tandem to probe the gas-phase conformation of selected cationised species from the block and random copolymers. The cross-sections established from these measurements and calculations have been shown to be dependent on molecular weight of the oligomer and radii of the cation but largely independent of the sequence of the ion in the gas-phase. The ion mobility results have been used to aid the understanding of the fragmentation of these copolymers by means of ESI-MS/MS.

Keywords: Oligomer; Ion mobility; ESI-MS/MS

1. Introduction

Copolymers of ethylene oxide (EO) and propylene oxide (PO) form an important class of modern industrial surfactant. These materials are used as dispersants, emulsifiers and stabilisers for pigments, dyestuffs, printing inks, paints, coatings, agricultural chemicals and lubricants [1]. They are widely used in pharmaceutical, medical, food and pesticide formulations. The performance of these materials depends on a number of factors. These include:

- Molecular weight distribution
- Initiator and/or terminator (end groups)
- Balance between hydrophobic PO chain and hydrophilic EO chain
- Random or block nature of copolymer

The successful commercial application depends on tailoring the required physical performance from the structure of the material. It is important, therefore, to be able to characterise the detailed microstructure of these materials and relate this information to physical properties.

The structure of the copolymer systems characterised in this study is shown below (**1**) where R indicates the initiating (α) end group and *x* and *y* are the number of moles of EO and PO, respectively. The initiator was a mixture of tridecanol and pentadecanol, which leads to formation of oligomers with tridecyl and pentadecyl initiating (α) end groups (R).

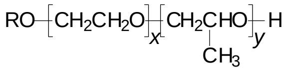

$$\mathrm{RO}\!-\!\left[\mathrm{CH_2CH_2O}\right]_x\!-\!\left[\mathrm{CH_2}\underset{\displaystyle \mathrm{CH_3}}{\underset{|}{\mathrm{C}}}\mathrm{HO}\right]_y\!-\!\mathrm{H}$$

1

Spectroscopic approaches such as infra-red (IR) spectroscopy and nuclear magnetic resonance (NMR) spectroscopy

---

[*] Corresponding author. Tel.: +44 1642 435720; fax: +44 1642 435777. *E-mail address:* tony_jackson@ici.com (A.T. Jackson).

[1] Present address: Department of Biological Sciences, The University of Warwick, Coventry CV4 7AL, UK.

1387-3806/$ – see front matter © 2004 Elsevier B.V. All rights reserved.
doi:10.1016/j.ijms.2004.09.025

have been used to characterise these polymer systems [2–8]. These approaches measure overall average values rather than individual molecular structure. In recent years, mass spectrometry has shown great promise in the provision of detailed molecular structural information from such low molecular weight polymeric systems [9]. For polymers of low polydispersity accurate molecular weight distributions can be obtained by using matrix-assisted laser desorption/ionisation (MALDI) mass spectrometry. Product ion spectra have also been obtained from selected precursor ions in the MALDI, or electrospray ionisation (ESI) mass spectrum of these materials, using collision-induced dissociation (CID) with the results interpreted to give valuable structural information [10–13]. EO/PO copolymer systems have been studied using these, and similar, approaches [14] and characteristic fragmentation mechanisms of polyethers have been outlined [14–18]. Polyether copolymers have also recently been studied by a combination of Fourier-transform mass spectrometry (FTMS) and electron capture dissociation (ECD) [19].

In order to better understand structure–property relationships in synthetic polymer systems an approach, based on ion mobility mass spectrometry, has been developed [20]. The technique of ion mobility mass spectrometry is based on the principle that ions with different conformations will have different mobilities when drifting through a buffer gas under the influence of a weak electric field. Theoretical approaches are then used to generate candidate structures of the ions and calculate their corresponding mobilities for comparison to experiment. This approach has been used to better understand cationisation of polymer molecules in the gas-phase and to probe gas-phase conformation [21–25]. This work involves detailed structural analysis of the copolymer systems combined with gas-phase conformational studies utilising the ion mobility mass spectrometry approach. The combination of the ion mobility studies with results from tandem mass spectrometry (MS/MS) has previously been found to aid the understanding of the latter experiment, especially with regard to the fragmentation mechanisms of polymers [21,25]. This combination of approaches has therefore been undertaken to facilitate the generation of structural information from the EO/PO copolymers involved in this study.

2. Experimental

Structural studies were carried out using electrospray ionisation (ESI) mass spectrometry and tandem mass spectrometry (MS/MS), acquired in a Q-ToF Ultima instrument (Waters MS Technologies, Manchester, UK). Ethylene oxide/propylene oxide (EO/PO) block and random copolymers were manufactured in-house (ICI). Exact mass MS/MS data were generated in the Q-ToF Ultima operating in 'W' optic mode at a resolution of approximately 20,000 (FWHM), with a Lockspray^{TM} source fitted. Lithium bromide (1%, v/v) was added to the sample (in 50/50, v/v methanol/water) to promote ionisation. Lithiated precursor ions (i.e., $[M+Li]^+$) have been found to provide optimal structural information [17].

Ion mobility mass spectrometry experiments were performed using a home-built MALDI-time of flight (MALDI-ToF) instrument. The details concerning the experimental set-up for the mass spectrum and ion mobility measurements have been published previously [26], so only a brief description will be given. Sodiated EO/PO copolymer ions (i.e., $[M+Na]^+$) were formed by MALDI in a home-built ion source. The matrix employed was 2,5-dihydroxybenzoic acid (DHB) and methanol was the solvent. Approximately 50 μL of DHB (100 mg/mL) and 50 μL of copolymer (1 mg/mL) were combined and 8 μL of NaI (saturated in methanol) was added to ionise the copolymer. The solution was then applied to the sample target and dried. A nitrogen laser ($\lambda = 337$ nm, 12 mW power per pulse) was used to generate ions in the MALDI source. To obtain a mass spectrum the ions were desorbed into a two-section (Wiley-McLaren) ion source and accelerated down a 1-m flight tube with 9 kV acceleration voltage. The MALDI-ToF is operated in reflectron mode to obtain high-resolution mass spectra.

For ion mobility experiments, the reflector is turned off and the ions are decelerated and gently injected into a drift cell at ∼300 eV. The glass drift cell is 20-cm long and filled with ∼1.5 Torr of helium gas. The temperature of the drift cell can be varied from 80 to 500 K depending on the needs of the experiment. A weak uniform electric field is applied across the cell that gently pulls the ions through the helium gas at a constant drift velocity. After exiting the drift cell, the ions are gently accelerated through a quadrupole mass filter, mass selecting the ion of interest to be detected with an electron multiplier. The quadrupole is set to a specific mass-to-charge ratio (m/z) to eliminate any ions that might arise from fragmentation in the drift cell and interfere with the ion mobility experiments. The pulse source extraction voltage triggers a timing sequence so that the ions are detected as a function of time, yielding an arrival time distribution (ATD). The mobility, K_o, of the ion is accurately determined from a series of arrival time distributions measured at different electric field strengths (7.5–16 V/cm) across the drift cell. Using kinetic theory, the ion's collision cross-section can also be determined.

3. Results and discussion

3.1. Tandem mass spectrometry of copolymers

The EO/PO polymers studied (**1**) were prepared from a mixed C_{13} and C_{15} alcohol initiator. Both block and random copolymers were available (Sample A and Sample B, respectively). The composition of the copolymers was confirmed by means of NMR measurements (data not shown) and was found to correspond to the results shown in Table 1.

Fig. 1 shows the ESI-MS spectrum obtained from Sample A. A large number of components are present, as expected,

Table 1
Sample details for copolymers studied

Sample	Initiator alcohol	EO (mol%)	PO (mol%)	Copolymer type
A	C_{13}/C_{15}	3	5	Block
B	C_{13}/C_{15}	12	5	Random

and the average molecular weight calculated from the ESI-MS spectrum is in reasonable agreement with that obtained from NMR. The predominant peaks are from singly charged $[M+Li]^+$ ions although some doubly charged $[M+2Li]^{2+}$ ion peaks are also observed (see annotation in Fig. 1). The ESI-MS spectra become more complex for higher molecular weight EO/PO copolymers, as a consequence of overlapping distributions from multiply charged ion peaks (from copolymers that are already very complex). The MALDI-ToF spectra from these copolymers (data not shown) are dominated by peaks from singly charged ions, even for the oligomers of highest molecular weights. The overlapping distributions of peaks from oligomers with different initiating (α) end groups (i.e., from the tridecanol and pentadecanol mixtures of alcohols used as the initiator for the copolymers) mean that deconvolution of the data would be required for three-dimensional intensity plots to be produced, as previously shown for other copolymers (also from MALDI-ToF data) [27–30].

The ESI-MS/MS product ion spectrum from a lithiated oligomer ($[M+Li]^+$) of Sample A (block copolymer) that contains three moles of EO reacted onto the tridecanol initiator, followed by four moles of PO (i.e., **1**, where x is 3, y is 4 and R is $–C_{13}H_{27}$), is displayed in Fig. 2. Some of the peaks in Fig. 2 have been annotated with proposed assignments. Proposed fragmentation schemes for polyglycols were established by Lattimer and coworkers [14,16], along with propounded mechanisms. A slightly modified (for the glycols characterised in these experiments) summary of some of these proposed fragmentation pathways is shown in Scheme 1. Ion peaks from each of the **A** (i.e., **A′** and **A″**), **B** (i.e., **B′** and **B″**) and **C** (i.e., **C′** and **C″**) series of fragment ion peaks described by Lattimer are observed in the spectrum displayed in Fig. 2. Only peaks from the **A′** and **A″** series are annotated in Fig. 2 for simplicity. This is also the case for annotation of all the other ESI-MS/MS spectra discussed here (vide infra). The annotation uses $\mathbf{C_{13}}$ to refer to the initiator (α) end group and $\mathbf{E}_n$ and $\mathbf{P}_n$ represent the units (n) of EO and PO, respectively. The ion peaks of the **A′** and **A″** series are not always more intense than that of the other series. Some of the peaks from the **C′** series are slightly more intense than their analogues from the **A′** series (i.e., compared to peaks from the **A′** series annotated as $\mathbf{C_{13}E_3}$, $\mathbf{C_{13}E_3P}$ and $\mathbf{C_{13}E_3P_2}$ in Fig. 2). Peaks from the **B′** and **B″** series are generally of much lower intensity than those from the **A′** and **A″** series.

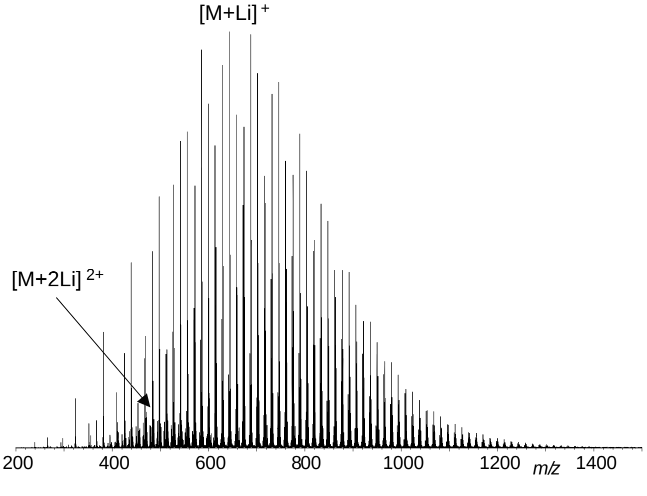

Fig. 1. ESI-MS spectrum of block EO/PO copolymer, Sample A, showing presence of both singly charged ($[\mathbf{1}+Li]^+$) and doubly charged ($[\mathbf{1}+2Li]^{2+}$) peaks from intact oligomers.

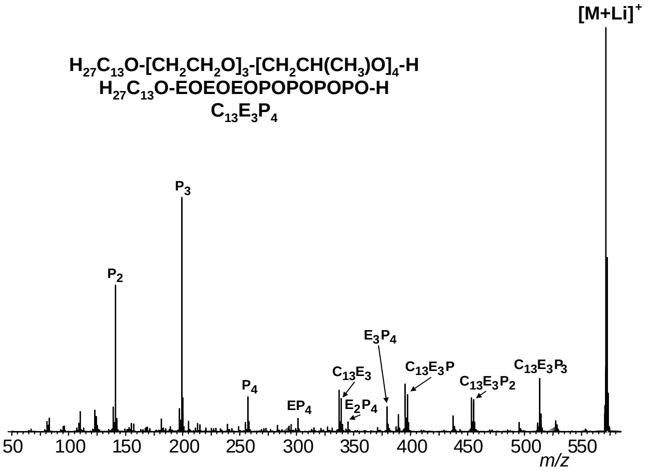

Fig. 2. ESI-MS/MS spectrum from the lithiated ($[\mathbf{1}+Li]^+$) tridecanol initiated block copolymer oligomer of Sample A, containing three units of EO and four units of PO. Peaks from the **A′** and **A″** series are annotated as described in the text.

These data are consistent with this oligomer being from a block copolymer, as is indicated by the proposed fragmentation of this moiety that is shown in Scheme 2. This scheme is annotated as for the fragment ion peaks in the ESI-MS/MS spectrum displayed in Fig. 2. Cleavage of the polymer backbone, with charge retention of the lithium cation, allows a full sequence of the oligomer to be generated from the product ion spectrum. The fragmentation is consistent with the block copolymer having been synthesised by addition of the EO to the tridecanol initiator prior to addition of PO. Peaks from the **A′** series indicate that this oligomer is terminated with PO units, as sequential units of this monomer are the difference between the highest m/z moieties (i.e., see $\mathbf{C_{13}E_3}$, $\mathbf{C_{13}E_3P}$, and $\mathbf{C_{13}E_3P_2}$ and $\mathbf{C_{13}E_3P_3}$ in Fig. 2 and Scheme 2). The **A″** series of peaks also suggest that this is the case. In addition, peaks from this series indicate that the EO is the first monomer feed added to the initiator, as losses of part of the initiator ($\mathbf{E_3P_4}$) and the initiator and EO units ($\mathbf{E_2P_4}$, $\mathbf{EP_4}$ and $\mathbf{P_4}$) are part of this series. This series also suggests that there is a run of PO units in this oligomer (i.e., peaks annotated as $\mathbf{P_2}$, $\mathbf{P_3}$ and $\mathbf{P_4}$ in Fig. 2 and Scheme 2).

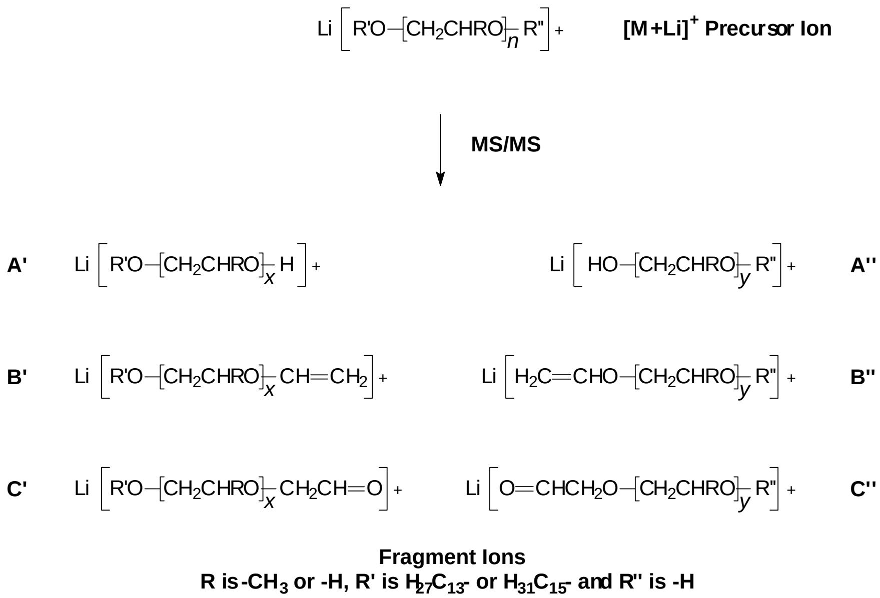

Scheme 1. Proposed fragmentation scheme for formation of the **A**′, **A**″, **B**′, **B**″, **C**′ and **C**″ series of ions from the EO/PO copolymers employed in this study.

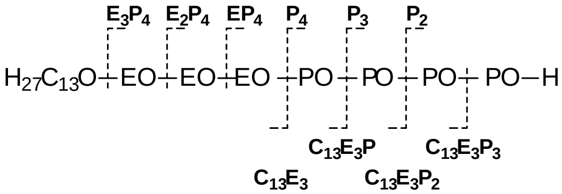

Scheme 2. Proposed fragmentation scheme for the lithiated ([**1** + Li]$^+$) tridecanol initiated block copolymer oligomer of Sample A, containing three units of EO and four units of PO.

The accurate mass assignments of the peaks, from the **A**′ and **A**″ series annotated in Fig. 2, are shown in Table 2. There is excellent agreement between the experimental and calculated mass-to-charge ratios, validating the assignments from the ESI-MS/MS data for this oligomer. These data enable confirmation of the initiator, indicating that tridecanol is indeed used, as many of the fragment ions retain this end group (e.g., $C_{13}E_3P_3$) and indicates that the sequence assignments are correct.

The ESI-MS spectrum from Sample B (data not shown) extends too much higher *m*/*z* than that from Sample A, as a consequence of the higher average molecular weight of the former copolymer. Singly charged peaks (i.e., from [M + Li]$^+$ ions) from the same lower molecular weight oligomers were observed in both spectra, however, so a comparison between ESI-MS/MS data obtained from the block (Sample A) and random (Sample B) copolymers was undertaken. The ESI-MS/MS spectrum, from a lithiated oligomer ([M + Li]$^+$) with the same empirical formula as that selected for the spectrum shown in Fig. 2, is displayed in Fig. 3. This precursor was

Table 2
Accurate mass results for ESI-MS/MS spectrum of lithiated tridecanol initiated block oligomer containing three units of ethylene oxide and four units of propylene oxide

Experimental, *m*/*z*	Calculated, *m*/*z*	Error, *m*/*z* (ppm)	Empirical formula	Assignment
141.1099	141.1103	−2.8	$C_6H_{14}O_3Li$	P_2
199.1520	199.1522	−0.8	$C_9H_{20}O_4Li$	P_3
257.1937	257.1940	−1.3	$C_{12}H_{26}O_5Li$	P_4
301.2200	301.2202	−0.8	$C_{14}H_{30}O_6Li$	EP_4
339.3080	339.3087	−2.0	$C_{19}H_{40}O_4Li$	$C_{13}E_3$
345.2467	345.2465	0.7	$C_{16}H_{34}O_7Li$	E_2P_4
389.2730	389.2727	0.8	$C_{18}H_{38}O_8Li$	E_3P_4
397.3506	397.3505	0.2	$C_{22}H_{46}O_5Li$	$C_{13}E_3P$
455.3924	455.3924	0.0	$C_{25}H_{52}O_6Li$	$C_{13}E_3P_2$
513.4340	513.4343	−0.5	$C_{28}H_{58}O_7Li$	$C_{13}E_3P_3$
		Mean = 1 ppm		

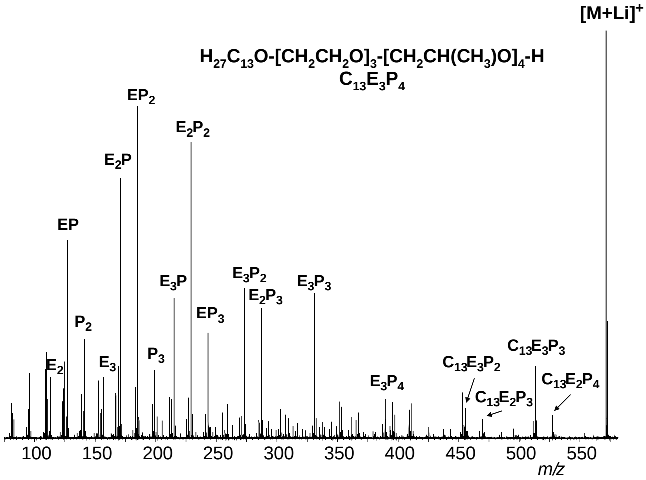

Fig. 3. ESI-MS/MS spectrum from the lithiated ([**1** + Li]$^+$) tridecanol initiated random copolymer oligomers of Sample B, containing three units of EO and four units of PO. Peaks from the **A**′ and **A**″ series are annotated as described in the text.

therefore expected to contain a tridecanol initiated random oligomer containing 3 mol of EO and 4 mol of PO (i.e., **1**, where x is 3, y is 4 and R is $–C_{13}H_{27}$). The spectrum is partially annotated with proposed assignments of the fragment ion peaks, as in Fig. 2. The spectrum from the random copolymer (Sample B, Fig. 3) is far more complex than that from the block material (Sample A, Fig. 2), as would be expected. The random oligomer would be expected to have up to 35 (i.e., [7!/4!3!]) isomers present at varying concentrations, depending on the degree of randomisation of the monomers during polymerisation. This would partially be dependant on the reactivity ratios of the two monomers with the tridecanol initiator and the growing oligomers.

The data indicate that the monomers are randomised along the oligomer chain, but that there may be a preference for an initial mole of PO to react with the initiator, rather than EO, prior to reaction randomly with additional monomers. Peaks of the **A**″ series from the last two (i.e., $\mathbf{E_2}$, **EP** and $\mathbf{P_2}$), three (e.g., $\mathbf{E_2P}$ and $\mathbf{EP_2}$), four (e.g., $\mathbf{E_3P}$, $\mathbf{E_2P_2}$ and $\mathbf{EP_3}$) and five monomer units (e.g., $\mathbf{E_3P_2}$ and $\mathbf{E_2P_3}$) indicate that the monomer units are fully randomised at the terminating end of the oligomer. There is, however, only a very low intensity peak for fragments of the **A**″ series, containing five and six monomer units of EO and PO, with four units of PO present. Indeed, two fragment ion peaks of this series (i.e., $\mathbf{E_2P_4}$ and $\mathbf{E_3P_3}$) having six monomer units would be expected to be close to equivalent intensity if addition of the first monomer unit of either EO or PO to the initiator was totally random. The peak from three units of both EO and PO, however, dominates in this region, which indicates that reaction of one unit of PO with the initiator is the principal reaction to start the growing oligomer chain.

These data clearly show that there are significant differences between product ion spectra that enable differentiation between block and random oligomers of these EO/PO copolymers. The more complex nature of the spectrum from the random copolymer (Sample B) clearly differs from that obtained from the block copolymer (Sample A), from which one dominant isomer is proposed to be present as expected.

A singly charged precursor ion ($[M + Li]^+$) from an oligomer of higher molecular weight from Sample A (block copolymer) was then selected for study. The resulting product ion spectrum, from an oligomer initiated with tridecanol and containing five units of EO and seven units of PO, is displayed below in Fig. 4. A similar pattern of fragment ion peaks is observed as from the lower molecular weight oligomer that is discussed above (see Fig. 2). The annotation used in this spectrum is analogous to that described above, modified from that initially proposed by Lattimer and coworkers [14,16]. The peaks annotated are again from the **A**′ and **A**″ series (see Scheme 1).

These data are again consistent with this oligomer from Sample A being a tridecanol initiated material that has been reacted with EO followed by PO to make a block copolymer. The proposed fragmentation for this oligomer is described in Scheme 3, in which the annotation is the same as that employed for the peaks of the **A**′ and **A**″ series in Fig. 4. This fragmentation scheme indicates that a full sequence of this block copolymer can be obtained from the ESI-MS/MS spectrum. The accurate mass results are again confirmatory with these assignments. They enable a more definitive knowledge of the structure of the initiator and the sequence information to be gleaned from the spectrum.

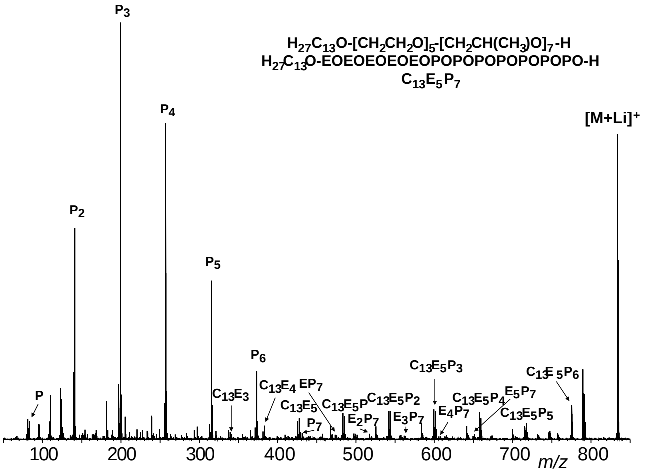

Fig. 4. ESI-MS/MS spectrum from the lithiated ($[\mathbf{1} + Li]^+$) tridecanol initiated block copolymer oligomer of Sample A, containing five units of EO and seven units of PO. Peaks from the **A**′ and **A**″ series are annotated as described in the text.

The pentadecanol initiated oligomers in Sample A are proposed to be present in significantly lower amounts than those originated from tridecanol, as the latter is present in significantly higher abundance in the original alcohol mixture used to make this material. Furthermore, some of the oligomers initiated with tridecanol will have the same empirical formula as those initiated with pentadecanol (e.g., an oligomer initiated with tridecanol, reacted with one unit of EO and five units of PO has the same empirical formula as a pentadecanol initiated oligomer containing three units of EO and three units of PO). It is possible, however, to select an oligomer from this sample for study by ESI-MS/MS that is purely initiated with pentadecanol, providing the EO content is low. The peak from one such oligomer has been used to generate the spectrum shown in Fig. 5. The singly charged, lithiated, precursor ion was from an oligomer initiated with pentadecanol, which had been reacted with one unit of EO and four units of PO. The annotation of the peaks from the **A**′ and **A**″ series, derived from the proposed fragmentation described by Lattimer and coworkers [14,16], is analogous to that from the tridecanol initiated oligomers (vide supra). The major difference is for the annotation of peaks from the **A**′ series, where $\mathbf{C_{15}}$ represents the initiator (α) end group of the oligomer.

The proposed fragmentation from this precursor is displayed in Scheme 4, with the annotation the same as that for peaks in the product ion spectrum shown in Fig. 5. This fragmentation allows full sequence of this oligomer from Sample A, again indicating that it is block copolymer. The accurate

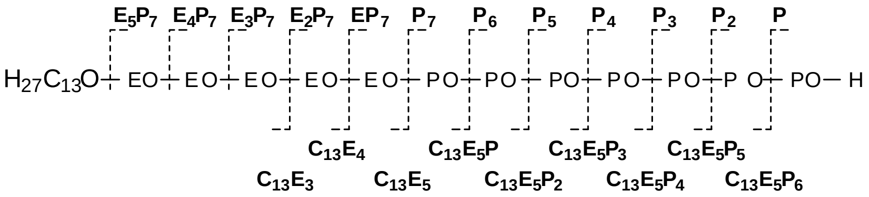

Scheme 3. Proposed fragmentation scheme for the lithiated ([**1** + Li]$^+$) tridecanol initiated block copolymer oligomer of Sample A, containing five units of EO and seven units of PO.

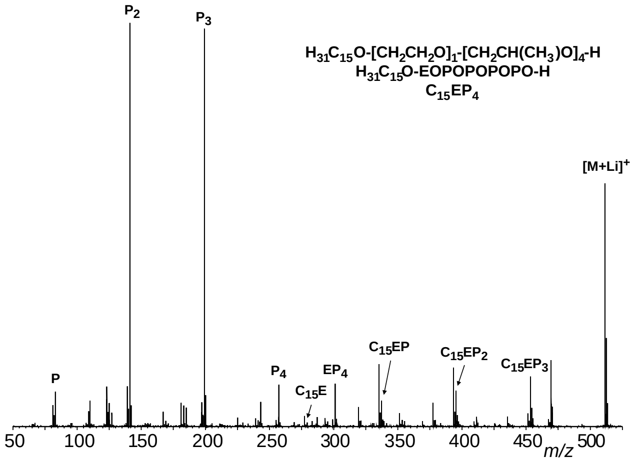

Fig. 5. ESI-MS/MS spectrum from the lithiated ([**1** + Li]$^+$) pentadecanol initiated block copolymer oligomer of Sample A, containing one unit of EO and four units of PO. Peaks from the **A**′ and **A**″ series are annotated as described in the text.

mass results aid confirmation of the structure of the initiator (α) end group, indicating that this oligomer was indeed initiated with pentadecanol. The fragmentation is consistent with reaction of one unit of EO with the initiator, followed by four units of PO, during synthesis of this oligomer of the block copolymer. These data indicate that the ESI-MS/MS experiment can be employed to differentiate between oligomers initiated with either tridecanol or pentadecanol, as well as aiding discrimination between block and random copolymers.

These studies, along with those from other copolymer systems [13], clearly show the power of the ESI-MS/MS approach in obtaining considerable structural information on random and block copolymers. Random and block species may be differentiated, information on the initiator and terminating agent may be generated and, in many cases, the complete sequence can be obtained for a block copolymer.

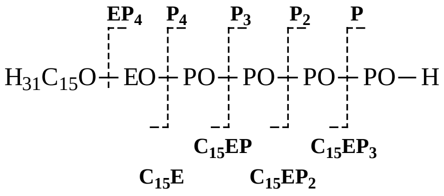

Scheme 4. Proposed fragmentation scheme for the lithiated ([**1** + Li]$^+$) pentadecanol initiated block copolymer oligomer of Sample A, containing one unit of EO and four units of PO.

The high sensitivity of the approach enables the acquisition of MS/MS data from minor components in copolymer samples. Exact mass MS/MS data aids end group identification and provides further confirmation of the proposed fragmentation mechanisms.

3.2. Ion mobility mass spectrometry results

Having obtained the detailed structural information from these samples, ion mobility experiments were carried out in order to probe the potential conformational changes. The data obtained can be analysed following the procedure described below.

The reduced mobility of the mass-selected ions can be obtained from the ATD using Eq. (1) [31]:

$$K_\mathrm{o} = l^2 \left(\frac{273}{760T}\right)\left(\frac{p}{V}\right)\left(\frac{1}{t_\mathrm{A} - t_\mathrm{o}}\right) \tag{1}$$

where l is the length of the cell, T is the temperature in Kelvin, p is the pressure of the He gas (in Torr), V is the potential, t_A is the ions' arrival time taken from the centre of the ATD peak and t_o is the amount of time the ion spends outside the drift cell before reaching the detector. A series of arrival times (t_A) are measured by changing the voltage (V) applied to the drift cell. A plot of t_A versus p/V yields a straight line with a slope inversely proportional to K_o and an intercept of t_o. Once K_o is found, the ion's collision cross-section can be obtained using Eq. (2):

$$\Omega^{(1,1)} = \frac{3e}{16N_\mathrm{o}}\left(\frac{2\pi}{\mu k_\mathrm{b} T}\right)^{1/2}\frac{1}{K_\mathrm{o}} \tag{2}$$

where e is the charge of the ion, N_o is the number density of He at STP, T is temperature, k_b is Boltzmann's constant and μ is the ion-He reduced mass [31].

3.3. Theoretical modeling

Conformational analysis of the ions is obtained by comparing the experimental cross-section from the arrival time distributions to the cross-sections of theoretical structures. Molecular mechanics/dynamics methods are required to generate trial structures for the EO/PO copolymers. Success has been achieved in using the AMBER set of molecular mechanics/dynamics programs [32] to provide reliable structures for many oligonucleotides [33–35]. In these cases, the theoretical cross-sections agreed well with the ion mobility data.

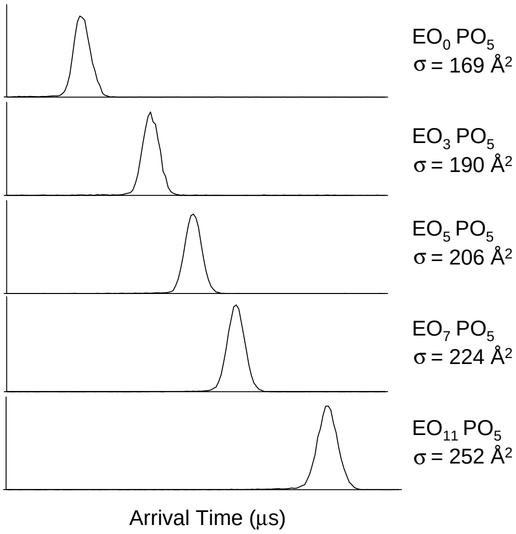

Fig. 6. Typical arrival time distributions for sodiated ([**1** + Na]$^+$) tridecanol initiated block copolymer oligomers, where the number of PO units is constant (y is 5) and EO units vary (x is 0, 3, 5, 7 and 11), from Sample A at 300 K.

Using the appropriate AMBER parameters, trial structures were calculated for sodiated EO/PO copolymers. An annealing/energy minimisation cycle was used to generate 100 structures for each copolymer. In this cycle, an initial minimisation of the structure is followed by 30 ps of molecular dynamics at 600 K and 10 ps of molecular dynamics in which the temperature is incrementally dropped to 0 K. The resulting structure is then energy minimised again and used as the starting structure for the next minimisation/dynamics run. After all low-energy structures are obtained, theoretical cross-sections must be calculated for comparison with experimental cross-sections. A temperature-dependent projection model [36,37], with appropriate atomic collision radii calculated from the ion–He interaction potential, is used to calculate the angle-averaged collision cross-section of each theoretical structure. A scatter plot of cross-section versus energy is collected for the minimised structures and used to help identify the ions observed in the experimental arrival time distributions.

3.4. Ion mobility results

Only one peak appears in the 300 K arrival time distributions obtained for all sodiated singly charged ([M + Na]$^+$) tridecanol initiated EO/PO oligomers from the copolymers (see data from block copolymer, Sample A, in Fig. 6). Single, symmetric peaks on arrival time distributions generally indicate that either one family of conformers is present or multiple conformers are present that rapidly interconvert in the drift cell. A single peak also appears in all the sodiated EO/PO arrival time distributions measured at a drift cell temperature of 110 K (which should be a low enough temperature to slow down most isomerisation processes and separate multiple conformers [35,38]). It is, therefore, likely that all of the possible sequences for the EO/PO oligomer have a similar conformation, allowing only one peak to occur in the gas-phase. The experimental collision cross-sections for sodiated tridecanol initiated block EO/PO copolymer oligomers of **1** [where the number of moles of EO(x) and PO(y) varies], obtained from the 300 K arrival time distributions, are listed in Table 3. The overall cross-sections, as expected, increase with increasing molecular weight of the EO/PO oligomers. There is excellent agreement between the experimental ion mobility values and those theoretical values calculated using the above approach.

Table 3
Experimental and theoretical cross-sections for sodiated block EO/PO copolymer (Sample A) oligomers

Block copolymer structure		Cross-section	
Units of EO	Units of PO	Experiment (Å^2)	Theory (Å^2)
5	3	186	188
5	5	206	205
5	7	228	230
0	5	169	171
3	5	190	193
5	5	206	205
7	5	224	223
11	5	252	253

The lowest energy structures calculated from some selected sodiated precursor ions, and their agreement with experimentally derived cross-sections, are shown in Fig. 7. All six oxygen atoms are shown to be coordinated with sodium cation for the oligomer containing no EO (i.e., homopolymer), with the other two oligomers (block copolymer) having seven coordinating oxygens. It is noted that these lowest energy confirmations indicate that the cation favours interaction primarily with the oxygen atoms at the terminating (ω) end of the latter two oligomers, which are from PO units for the block copolymer (Sample A). This coordination is, therefore, with oxygens that are predominantly the furthest away from the alkyl chain of the tridecanol initiator. Previous results from poly(ethylene glycol) (PEG) [24,39–41] and poly(propylene glycol) (PPG) [24] indicated that the coordination of sodium ions with oligomers was similar to that shown in Fig. 7, with the cation efficiently wrapping the polymer around it (i.e., to ‘solvate’ the cation as for crown ethers). These previous studies showed that oligomers had preferential conformers with the sodium cation that involved coordination with either seven or eight oxygen atoms for PPG and PEG, respectively [24]. It was discovered for polyethers that there was a competition between the sodium cation and the polyether backbone that influenced the overall conformation, such that less oxygen atoms coordinated to the PPG which has an extra methyl group in the monomer unit compared to PEG. The coordination number with the sodium cation, for the EO/PO oligomers, is the same as that for PPG oligomers. This might be expected as most of the oxygens coordinated to the sodium ion, for these block copolymer oligomers, are from the PO units.

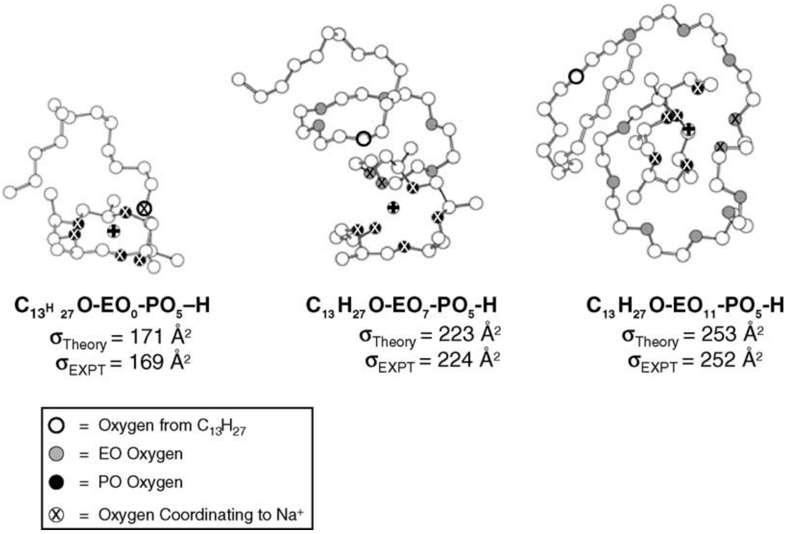

Fig. 7. Lowest energy structures for sodiated ($[\mathbf{1} + \mathrm{Na}]^+$) tridecanol initiated block copolymer oligomers, where the number of PO units is constant (*y* is 5) and EO units vary (*x* is 0, 7 and 11). Experimental and theoretical cross-sections (Å^2) for these oligomers are also shown.

Table 4 shows the cross-sections calculated from the arrival time distributions measured for selected tridecanol initiated sodiated precursors from the block (Sample A) and random (Sample B) EO/PO copolymers. The striking observation here is that the calculated cross-sections for the block and random copolymer molecules are virtually identical. This would suggest that, for sodiated ions in the gas-phase, that differing structural isomers of an EO/PO oligomer ion have little effect on the observed arrival time in the ion mobility experiment for that species and thus the calculated cross-section. In order to try to understand this result, theoretical calculations of the lowest energy structures for some isomers were generated. Fig. 8 shows a typical result for the sodiated ions formed from precursors of tridecanol initiated oligomers containing five units of both EO and PO. Two of these structures are from block copolymer oligomers, but differ in the monomer that is reacted with the initiator first. The third lowest energy structure is from an alternating EO/PO oligomer. As can be seen from the structures even these significant changes in composition lead to no difference in the calculated cross-sections. All three lowest energy structures have the sodium ion coordinated to seven oxygen atoms of the oligomer. This coordination number is the same even though the oxygen atoms are from different ratios of units of the two monomers, ranging from two to five PO units and two to five EO units. Furthermore, these oxygen atoms are all from the last seven units of monomer in the oligomeric chains, that is at the terminating (ω) end of the EO/PO copolymer. This is the same as seen for oligomeric chains from the block copolymer material (Sample A), as shown in Fig. 7. The cation does not appear to have an affinity for oxygen atoms near the hydrophobic alkyl chain at the initiator (α) end group.

Table 4
Experimental cross-sections for sodiated block (Sample A) and random (Sample B) EO/PO copolymer oligomers

Copolymer structure		Cross-section	
Units of EO	Units of PO	Block copolymer (experiment, Å^2)	Random copolymer (experiment, Å^2)
5	3	186	185
5	5	206	207
5	7	228	227
0	5	169	168
3	5	190	191
5	5	206	207
7	5	224	223
11	5	252	252

In order to probe the effect of the cation on the cross-sections, measurements were made on lithium, sodium, potassium and caesium cationised precursors of both the block (Sample A) and random (Sample B) EO/PO copolymers. Table 5 shows the experimental results obtained from block and random cationised precursors that were tridecanol initiated with eleven units of EO and five units of PO. The results show, as might be expected, a small increase in experimental cross-section with increased size of cation but the results for the block and random samples with the same cation are virtually identical. There is, therefore, no observable differentiation between the cross-section of block and ran-

Table 5
Metal dependence of experimental cross-sections of sodiated tridecanol initiated block and random oligomers, containing 11 units of ethylene oxide and 5 units of propylene oxide

Metal cation	Cross-section	
	Block copolymer (experiment, Å^2)	Random copolymer (experiment, Å^2)
Li^+	251	251
Na^+	252	252
K^+	254	254
Cs^+	255	256

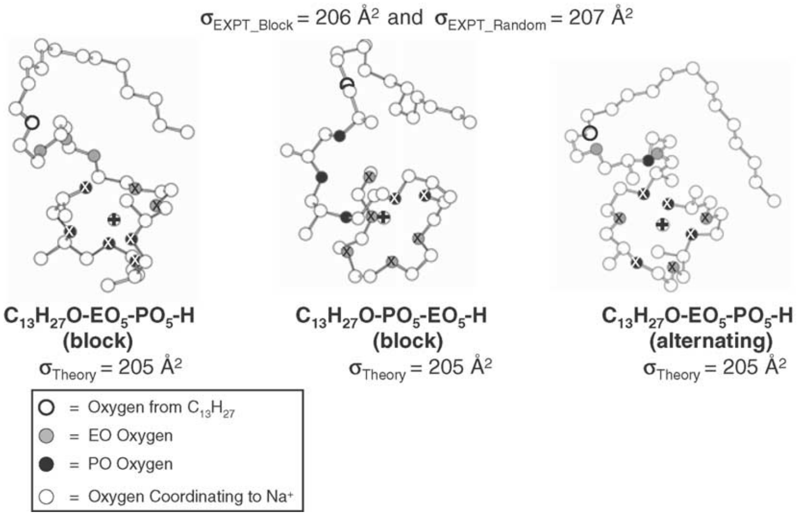

Fig. 8. Lowest energy structures for sodiated ($[\mathbf{1} + \mathrm{Na}]^+$) tridecanol initiated block and alternating copolymer oligomers, where the number of EO units is five (x is 5) and PO units is also five (y is 5). Theoretical cross-sections (Å^2) for these oligomers are also shown.

dom samples with increased size of cation. This observation is again supported by theoretical calculations. Typical lowest energy structures for block EO/PO oligomers, with lithium, potassium and caesium cations, are shown in Fig. 9. The coordination number of oxygen atoms to the cation increases, as expected, with increased radii of cation from six coordinate for the lithium ion up to 10 coordinate for the much larger caesium cation. A similar phenomenon was observed previously from other polyethers [24,41]. The calculated cross-sections agree well with the experimental results, as shown in Fig. 9. There is a significant difference in the location of the cation in the theoretical structures shown in Fig. 9, when comparing that with caesium to that with potassium and lithium ions. The cations interact with oxygens at the terminating (ω) end of the polymer chain, for lithium and potassium ions, whereas the caesium ion is coordinated to oxygens at the initiator (α) end of the oligomer. The former oxygens are therefore primarily from PO of the block oligomer, compared to the totally EO oxygen focussed caesium cation in the latter case.

The lowest energy structure for the lithium cation coordinating to the EO/PO copolymer (Fig. 9) could give some insight into the fragmentation in the ESI-MS/MS spectra of the block and random oligomers described above. The ESI-MS/MS spectra were all obtained from singly charged lithiated precursors. The fragment ion peaks in all of these spectra are far more intense for cleavages of the copolymer backbone occurring near to the terminating (ω) end of the oligomers. The mechanisms for formation of these fragment ions were

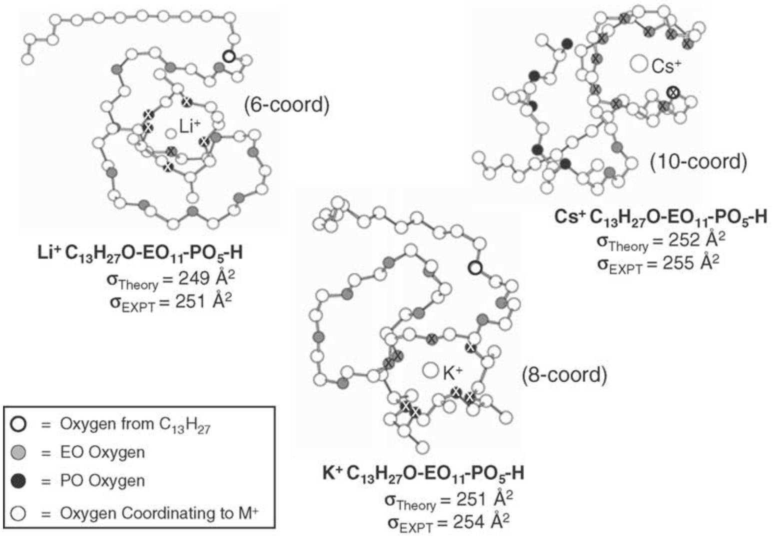

Fig. 9. Lowest energy structures for a cationised ($[\mathbf{1} + Cat]^+$), where *Cat* is a lithium, potassium or caesium ion, tridecanol initiated block copolymer oligomer, where the number of EO units is 11 (x is 11) and PO units is five (y is 5). Experimental and theoretical cross-sections (Å^2) for these oligomers are also shown.

previously proposed to be charge mediated [14,16]. The coordination of the lithium cation with the oxygen atoms that are closest to the terminating (ω) end of the oligomers would indicate that reactions, in the ESI-MS/MS experiment, involving cleavages close to these atoms would be most prevalent, leading to increased intensity for the lower *m*/*z* peaks from the $\mathbf{A}''$ series and the highest *m*/*z* peaks from the $\mathbf{A}'$ series. These are the peaks from cleavage at the terminating (ω) end of the EO/PO copolymers that are indeed observed as the most intense in the ESI-MS/MS spectra. These results do indicate that the mechanisms for formation of the fragment ions are charge induced, as proposed by Lattimer and coworkers [14,16].

4. Conclusions

The properties of EO/PO copolymers are thought to depend on initiator, molecular weight, molecular weight distribution and sequence. The bulk properties of these materials are often studied using physical methods or spectroscopic approaches such as NMR spectroscopy. Mass spectrometry, using ESI or MALDI as an ionisation method, has been shown to be a good method for establishing the average molecular weight and molecular weight distribution for systems of low polydispersity. This work has shown that, by utilising ESI-MS/MS data, and using accurate mass information where needed, the initiator molecule can be identified and the random or block nature of the molecule established. A complete sequence of the copolymer can be derived for the block EO/PO copolymer oligomers.

The conformation of the cationised molecule in the gas-phase can be studied by utilising ion mobility mass spectrometry approaches. The cross-section of the ion can be estimated by measuring the ion arrival times. Experimental and theoretical data may be compared utilising theoretical calculations, based on the AMBER set of molecular mechanics/dynamics programs. The experimental results were in good agreement with those obtained from theory, in all cases, giving confidence in the validity of the approach. The results showed that the cross-section of the selected ion increased with molecular weight and, to a lesser extent, with size of cation, but that the cross-section was independent of the sequence of the selected ion. Even ions having structures as different as block and alternating EO/PO copolymer oligomers gave essentially the same cross-section. These results indicate that, for cationised species in the absence of solvent, that the measured, and calculated cross-sections are independent of sequence. This indicates the importance of solvent interactions for these components since experimentally measured physical parameters of these materials in solution depend on sequence.

The combined structural/conformational approach adopted in this work has been shown to provide interesting complimentary data on EO/PO copolymers, indicating information about the fragmentation mechanisms involved in the ESI-MS/MS experiment, and could be applied to other polymeric systems to probe structure activity relationships.

References

[1] R.W. Body, V.L. Kyllingstad, Encyclopedia of Polymer Science and Engineering, vol. 6, John Wiley & Sons, Chichester, UK, 1986, p. 225.

[2] C.S. Kweon, D.W. Kim, H.K. Cho, S.T. Noh, J. Ind. Eng. Chem. 9 (2003) 146.

[3] P. Kipkemboi, A. Khan, B. Lindman, V. Alfredsson, Can. J. Chem. Rev. Can. Chim. 81 (2003) 897.

[4] A. Kelarakis, S.M. Mai, V. Havredaki, A. Brett, C.J. Booth, Colloid Interface Sci. 275 (2004) 439.

[5] Y.J. Huang, G.R. Qi, G.X. Chen, Chin. J. Polym. Sci. 20 (2002) 453.

[6] T. Hamaide, A. Goux, M.F. Llauro, R. Spitz, A. Guyot, Angew. Makromol. Chem. 237 (1996) 55.

[7] L.A. Goff, J. Soc. Cosmet. Chem. 48 (1997) 59.

[8] W. Gronski, Makrom. Chemie-Macrom. Chem. Phys. 192 (1991) 591.

[9] J.H. Scrivens, A.T. Jackson, Int. J. Mass Spectrom. 200 (2000) 261.

[10] A.T. Jackson, H.T. Yates, J.H. Scrivens, G. Critchley, J. Brown, M.R. Green, R.H. Bateman, Rapid Commun. Mass Spectrom. 10 (1996) 1668.

[11] A.T. Jackson, H.T. Yates, J.H. Scrivens, M.R. Green, R.H. Bateman, J. Am. Soc. Mass Spectrom. 8 (1997) 1206.

[12] A.T. Jackson, H.T. Yates, J.H. Scrivens, M.R. Green, R.H. Bateman, J. Am. Soc. Mass Spectrom. 9 (1998) 269.

[13] A.T. Jackson, S.E. Slade, J.H. Scrivens. Int. J. Mass Spectrom.238 (2004) 265.

[14] R.P. Lattimer, J. Am. Soc. Mass Spectrom. 5 (1994) 1072.

[15] R.P. Lattimer, H. Munster, H. Budzikiewicz, Int. J. Mass Spectrom. Ion Process. 90 (1989) 119.

[16] R.P. Lattimer, J. Am. Soc. Mass Spectrom. 3 (1992) 225.

[17] R.P. Lattimer, Int. J. Mass Spectrom. 116 (1992) 23.

[18] T.L. Selby, C. Wesdemiotis, R.P. Lattimer, J. Am. Soc. Mass Spectrom. 5 (1994) 1081.

[19] B.A. Cerda, D.M. Horn, K. Breuker, F.W. McLafferty, J. Am. Chem. Soc. 124 (2002) 9287.

[20] M.T. Bowers, P.R. Kemper, G. von Helden, P.A.M. van Koppen, Science 260 (1993) 1446.

[21] J. Gidden, A.T. Jackson, J.H. Scrivens, M.T. Bowers, Int. J. Mass Spectrom. 188 (1999) 121.

[22] J. Gidden, T. Wyttenbach, A.T. Jackson, J.H. Scrivens, M.T. Bowers, J.J. Batka, P.J. Weis, Am. Soc. Mass Spectrom. 10 (1999) 883.

[23] J. Gidden, T. Wyttenbach, A.T. Jackson, J.H. Scrivens, M.T. Bowers, J.J. Batka, P.J. Weis, Am. Chem. Soc. 121 (1999) 1421.

[24] J. Gidden, T. Wyttenbach, A.T. Jackson, J.H. Scrivens, M.T. Bowers, J. Am. Chem. Soc. 122 (2000) 4692.

[25] J. Gidden, A.T. Jackson, J.H. Scrivens, M.T. Bowers, J. Am. Soc. Mass Spectrom. 13 (2002) 499.

[26] E.S. Baker, J. Gidden, D.P. Fee, P.R. Kemper, S.E. Anderson, M.T. Bowers, Int. J. Mass Spectrom. 227 (2003) 205.

[27] G. Wilczek-Vera, Y.S. Yu, K. Waddell, P.O. Danis, A. Eisenberg, Macromolecules 32 (1999) 2180.

[28] G. Wilczek-Vera, Y.S. Yu, K. Waddell, P.O. Danis, A. Eisenberg, Rapid Commun. Mass Spectrom. 13 (1999) 764.

[29] G. WilczekVera, P.O. Danis, A. Eisenberg, Macromolecules 29 (1996) 4036.

[30] A.T. Jackson, J.H. Scrivens, W.J. Simonsick, M.R. Green, R.H. Bateman, Polym. Preprints 41 (2000) 641.

[31] E.A. Mason, E.W. McDaniel, Transport Properties of Ions in Gases, Wiley, New York, 1988.

[32] D.A. Case, D.A. Pearlman, J.W. Caldwell, T.E.C. III, W.S. Ross, C.L. Simmerling, T.A. Darden, K.M. Merz, R.V. Stanton, A.L. Cheng, J.J. Vincent, M. Crowley, V. Tsui, R.J. Radner, Y. Duan, J. Pitera, I. Massova, G.L. Seibel, U.C. Singh, P.K. Weiner, P.A. Kollman, AMBER 6.0 ed., University of California, San Francisco, 1999.
[33] J. Gidden, J.E. Bushnell, M.T. Bowers, J. Am. Chem. Soc. 123 (2001) 5610.
[34] J. Gidden, M.T. Bowers, J. Am. Soc. Mass Spectrom. 14 (2003) 161.
[35] J. Gidden, M.T. Bowers, Eur. Phys. J. D 20 (2002) 409.
[36] T. Wyttenbach, G. von Helden, J.J. Batka Jr., D. Carlat, M.T. Bowers, J. Am. Soc. Mass Spectrom. 8 (1997) 275.
[37] G. von Helden, M.T. Hsu, N. Gotts, M.T. Bowers, J. Phys. Chem. 97 (1993) 8182.
[38] J. Gidden, T. Wyttenbach, J.J. Batka, P. Weis, A.T. Jackson, J.H. Scrivens, M.T. Bowers, J. Am. Chem. Soc. 121 (1999) 1421.
[39] G. von Helden, T. Wyttenbach, M.T. Bowers, Int. J. Mass Spectrom. Ion Process. 146 (1995) 349.
[40] G. von Helden, T. Wyttenbach, M.T. Bowers, Science 267 (1995) 1483.
[41] T. Wyttenbach, G. von Helden, M.T. Bowers, Int. J. Mass Spectrom. 165 (1997) 377.